Advancing Therapeutic Efficacy of Star Anise Oil with (*Illicium verum*) Nano-Emulsion Formulation

Sharad Visht [1], Sana Sirwan Salih [1], Belan Azad Ibrahim [1], Daniah Issa Ismael [1], Serwa Falah Abdalwaheed [1], Omji Porwal [1]

Abstract

Background. The volatile oil present in star anise (*Illicium verum*) exhibits efficacy against various health issues such as bronchitis, colds, flu, indigestion, facial paralysis, and intestinal cramps. This study aimed to formulate and assess the nano-emulsion of star anise volatile oil. **Method.** Star anise volatile oil was extracted from its fruits using the Clevenger apparatus and subsequently purified. The extraction process involved dissolving the extracted oil in dichloromethane, and solvent recycling was performed using a rotavapor. Nano-emulsions were developed through homogenization (8 batches) and ultra-sonication methods (8 batches) with varying surfactant (Tween-80) and co-surfactant (PEG-200, PEG-300) ratios. Characterization involved refractive index, pH, Fourier transform infrared spectroscopy, particle size distribution, zeta potential, drug content, drug release, release kinetics, and stability studies (25˚C/60% RH at 1, 2, 3, 4, and 5 weeks). **Results.** The smallest droplet sizes were observed in batches NE-HH (646.1±71.54 nm) and NE-HS (694±195.48 nm), with the least zeta potential values of -10.4 mV (NE-FH batch) and -5.2 mV (NE-HS batches). The highest drug release percentages were recorded in NE-EH (31.411±1.26%) and NE-ES (34.004±1.74%) batches. Both NE-EH and NE-ES followed the Peppas Korsmeyer model, and the release mechanism was identified as Fickian Diffusion (Higuchi Matrix). **Conclusion.** The study concludes that nano-emulsions of star anise volatile oil can be successfully prepared using homogenization and ultrasonication methods, demonstrating good stability and prolonged drug release.

Keywords. Homogenization, ultrasonication, zeta potential, drug release, essential oil.

Significance | Star anise oil-based nano-emulsions' extraction, purification, and formulation processes to improve therapeutic efficacy of drug substances

*Correspondence. Dr. Sharad Visht, Assistant Professor, Department of Pharmaceutics, Faculty of Pharmacy, Tishk International University, Erbil, Kurdistan Region, Iraq. Mobile. +91-9719302784, E-mail. sharad.visht@tiu.edu.iq

Editor Md Shamsuddin Sultan Khan And accepted by the Editorial Board Jan 20, 2024 (received for review Nov 3, 2023)

1. Introduction

Nature exhibits remarkable diversity, and in the face of increasing disease outbreaks, people have sought relief from the vast array of plants concealed in Mother Nature's lap. For centuries, plants have been harnessed for medicinal purposes, tracing back to ancient cultures predating recorded history, serving both preventative and therapeutic roles (Habeeb Hiba and John E, 2022). Over the ages, this practice has evolved, leading to sophisticated methods of isolating active components and formulating more potent remedies (Elkordy et.al, 2021). Today, medicinal herbs are globally employed as standardized herbal extracts, extending beyond their traditional use in rural areas (Srivastava S. 2023).

Chemicals and essential oils are extracted from various plant parts, including flowers (Liao, 2021), barks (Hannou, 2022), seeds (Tokuma, 2020), roots (Barbouchi et.al, 2021), and fruits (Brahmi F. et.al, 2021), utilizing diverse techniques such as hydro distillation (Miljanović et.al., 2023) and Soxhlation (Sukasri et.al, 2023). Nano-emulsion formulations of essential oils, as explored

Author Affiliation.
[1] Department of Pharmaceutics, Faculty of Pharmacy, Tishk International University, Erbil, Kurdistan Region, Iraq.

Please cite this article.
Sharad Visht, Sana Sirwan Salih, Belan Azad Ibrahim et al., (2024). Advancing Therapeutic efficacy of Star Anise Oil with (Illicium verum) Nano-Emulsion Formulation, Journal of Angiotherapy, 8(1), 1-11, 9383

by Hitesh Chopra et.al (2022), are emerging as promising methods for efficiently administering active herbal constituents.

One widely used plant in the medical field is Star anise, also known as Chinese star anise (*Illicium verum*). This charming evergreen tree, belonging to the Schisandraceae family, is valued for both its culinary and medicinal purposes (Sharafan et.al., 2022). Originating from southern China and northern Vietnam (Salem et.al, 2021), it bears purple-red flowers that give way to distinct star-shaped fruits, possessing a unique anise scent and flavor. The pale-yellow essential oil extracted from star anise is employed in traditional medicine, incorporated into teas and herbal remedies to address various ailments. It's essential to note that the star-shaped fruits of *L. anisatum*, also called Japanese star anise, can be easily mistaken for those of *L. verum* (True star anise) due to their striking resemblance, leading to cases of adulteration between these two species in the late 1800s.

Regrettably, cases of mixing up or deceiving the two species have led to serious consequences, particularly regarding the Japanese star anise, which is highly toxic (Salem et.al., 2021). The toxicity of Japanese star anise is attributed to its elevated levels of anisatin, a neurotoxic compound causing seizures and other neurological disorders if ingested (Zou et.al., 2023). Due to concerns about its toxicity, the FDA has issued a warning against consuming "teas" made from star anise, highlighting the risk of potential adulteration (Patil et.al., 2023).

Traditionally, Star anise has been utilized in Chinese remedies and Asian and Indian cuisines, prized for its licorice scent and health benefits. Greeks and Romans used it for energy boost, while Chinese medicine employed it to alleviate muscle pain, induce vomiting, and improve sleep patterns. In Indian systems, it found use for dyspepsia, spasms, and dysentery. Star anise made its way to Europe in the 17th century, where it was introduced as an expectorant and spice.

The main components of star anise, anethole, and trans-anethole, contribute significantly to its biological effects, including antibacterial properties against various strains, antifungal abilities, as well as antioxidant and anti-inflammatory actions (AlBalawi et.al., 2023). Presently, these components are harnessed for body care support due to their potent aroma. When combined with a carrier oil, they can be topically applied to alleviate dry and itchy skin.

Star anise oil finds application as a diffuser and inhaler in treating bronchitis, the common cold, and flu. In aromatherapy, it aids digestion, eases muscle aches, and acts as a stress reliever. Recognized as a sedative, star anise oil is useful in calming the mind during anxiety conditions. Medicinal plants, such as star anise, play a crucial role in public health, with studies showing its effectiveness in reducing pro-inflammatory production with minimal side effects, thanks to its rich trans-anethole content (Majali, 2022).

Materials and Method

The dried star anise obtained from amazon (Tiptop Home Star Anise 500 g Buy Whole Foods Online Ltd.) obtained from the local herbal market in Erbil, Kurdistan, Iraq. The DMSO, Tween-80, PEG-20, PEG-300 obtained from FINKEM. The HCl, sodium bicarbonate, phosphate buffer pH 7.4 obtained from CDH Ltd. All chemicals used were of the analytical grades.

Extraction of Star Anise oil.

The hydro-distillation technique used to extract the essential oil from the dried star anise fruits as showed in **Figure-1**. Accurately weighed 750 g of dried star anise fruits crushed and filled into 5 L Round bottom flask filled with water up to ¾ volume of round bottom flask (RBF). The assembly runs for 6 h in 3 different batches. The oil was collected, and water was added to separate any fat / lipid (if present), using separating funnel and the non-aqueous phase was further purified (Mahmod et al., 2021; Miranda et al., 2022).

Purification of extracted Star Anise Oil.

The essential oil purified by mixing essential oil with dichloromethane (DCM) and the DCM layer separated using separating funnel. The separated mixture was placed in rotavapor to recycle the solvent from essential oil (Mahmod et al., 2021; Wong et al., 2014). After full DCM recycles the essential oil collected and stores in ampoules as showed in **Figure-1**.

Characterization of extracted Star anise oil

The yield, refractive index, density, FTIR, UV-visible spectroscopy of essential oil performed.

Yield. The yield (% v/w) calculated as per following formula ((Visht & Sirwan Salih, 2023))

$$Yield\ of oil\ (\%) = \frac{Volume\ of oil\ obtained}{Mass\ of leaves} X\ 100$$

Refractive Index of star anise essential oil.

The refractive index verifies the purity and concentration of the essential oil. The refractive index was measured by the Mettler Toledo 30PX refractometer by placing the 0.5 mL sample in the sample chamber and the results were displayed on the screen (Visht & Sirwan Salih, 2023)).

Density of oil. The Mettler Toledo DensitoPro is used to measure the density of essential oil. The filling tube was immersed into the samples to measure the density (Visht & Sirwan Salih, 2023)).

Fourier-transform infrared spectroscopy (FTIR).

Fourier-transform infrared spectroscopy conducted using the FTIR device (Shimazu, IRAffinity-1S) to find the functional groups and bonds present in sample by scanning between 500-4000 cm^{-1}. A drop of oil was placed on the IR window and FTIR was measured (Visht & T Kulkarni, 2016).

UV-visible spectrophotometry.

The UV-Visible spectrophotometer (Thermoscientific Genesys 180) used to prepare the calibration curve of drug to show the relation between concentration and absorbance to figure out the drug content and drug release study. The stock solution (1 mg/mL) was prepared in dimethyl sulfoxide (DMSO) and further dilutions (20, 40, 60, 80, 100, 120 µg/mL) were prepared and scanned at maximum absorbance (λ_{max}) ((Roberts et al., 2018; Rombaut et al., 2015).

Drug excipient interaction.

The drug excipient interaction was determined by FTIR. ((Visht & Sirwan Salih, 2023))

Preparation of Nano-emulsion from Star Anise Oil

The star anise oil-based nano-emulsion was prepared by using accurately weighed quantities of anise oil (dispersed oil phase) along with Tween-80 (surfactant) and PEG-200 and PEG-300 (co-surfactants) (Pires et.al., 2023). The nano-emulsion was prepared by two methods named; homogenization and ultrasonication and each method consists of eight batches based on their composition as showed in **Table-1** (Liang et al., 2023; Manzoor et al., 2023). The preparation of nano-emulsion involved mixing of oil, surfactant, and co-surfactant and the subjected to homogenization or sonication. The nano-emulsion batches involving use of two co-surfactants where the two co-surfactants mixed first and then added with oil and surfactant mixture and further subjected to homogenization or sonication. The ultrasonication time was 1 h using an ultrasonic bath (Elmasonic S100H Ultrasonic Cleaner) and homogenization time was 30 s using a high-performance homogenizer (IKA Ultra-Turrax T-25 Digital Homogenizer) as showed in **Figure-2** (Pratap-Singh et.al., 2021). The resulting nano-emulsion batches from both groups were transparent, monophasic, homogenous, stable liquid mixtures (Alhamdany et.2021; (Donsì et al., 2011; Zhang et al., 2021))

Characterization and evaluation of nano-emulsion

The nano-emulsions subjected for refractive index, pH, FTIR, particle size distribution, zeta potential, drug content, drug release, drug release kinetics, and their stability.

Refractive index.

The refractive index of the nano-emulsion formulations measured as mentioned before.

pH determination.

pH measurement is another essential parameter that must evaluated clearly because pH value finds stability and any change in this value affects zeta potential and showed presence of reaction that diminishes quality of your formulation. The experiment conducted in triplicate by using digital pH meter and results recorded.

FTIR.

The FTIR formulation was carried out to confirm interaction using a method to prepare nano-emulsion. (Dinache et al., 2020; Gurpreet & Singh, 2018)

Particle size analysis.

The Litesizer 500 (Anton Paar GmbH Company) was used to measure the droplet size of nano-emulsion as droplet size plays a key role in distribution and absorption of drug (Zhang et al., 2022). The results of all sixteen batches are tabulated in Table-3. The 2 drops of nano-emulsion were placed in single- use plastic cuvette and diluted with de-ionized water for accurate scanning (Visht & Sirwan Salih, 2023).

Zeta-potential.

The nano-emulsions, consisting of tiny droplets dispersed in a liquid medium, rely on zeta potential for stability. A high zeta potential, either positive or negative greater than 20 mV, fosters strong electrostatic repulsion between droplets, preventing their clumping and ensuring the emulsion stays stable. Conversely, a low zeta potential weakens the repulsive forces, leading to reduced physical stability and potential phase separation (Vilanculos et al., 2023). To determine the zeta potential of star anise oil nano-emulsion, the "Litesizer 500" (Anton Paar GmbH Company) was used (Pandey et al., 2023). The analysis began by preparing a dilute suspension of the nano-emulsion in deionized water with a concentration suitable for the instrument. The suspension was then loaded into the omega cuvette and placed in the measurement cell of the instrument. The zeta potential was then determined and recorded at a suitable pH and temperature. The results of all sixteen batches are tabulated in Table-3. (Visht & Sirwan Salih, 2023).

Drug content.

The 0.5 mL nano-emulsion was mixed with 4 mL of DMSO, and the absorbance was measured using UV-Visible spectrophotometer (Thermoscientific Genesys 180) to determine the drug content and results tabulated in Table-3. (Alaayedi & Maraie, 2023).

Drug release.

The drug release study was performed using the vertical diffusion cell (Copley Scientific, HDT 1000) at 35±0.5° C temperature. The receiver compartment filled with 10 mL phosphate buffer pH 7. The 0.5 mL of nano-emulsion is placed in donor compartment. The magnetic placed in the receiver compartment to confirm homogeneity in the system. The 3 mL of samples were taken and replaced with fresh buffer at different time intervals. All samples were scanned for UV to prepare a graph between time and percent cumulative drug release (Bayan et.al., 2023).

Drug release kinetics.

To study the release kinetics of various batches of nano-emulsions, the drug release data was computed in different kinetics model of (a) zero order (cumulative percent drug

released vs. time) (b) first order (Log cumulative percent drug retained vs. time) (c) Higuchi (Log cumulative percent drug released vs. square root of time) (d) Peppas release kinetics equation (Log of cumulative % release Vs log time). The regression coefficient values of different release kinetics equations were evaluated by computing the data of release profiles of optimized star anise nano-emulsion formulation (Rani et.al., 2022).

Stability.

The stability studies performed by weighed 1 mL of nano-emulsion placed in Petri dish at successive twenty-five-degree centre-grade at 60% RH at 1, 2, 3, 4 and 5 weeks.

Results

Characterization of extracted Star anise oil Various parameters like yield, refractive index, density, FTIR, UV-visible spectroscopy, drug content, and drug diffusion studies were conducted.

Yield of extracted Star anise oil.

The Star anise oil essential oil was successfully extracted and purified, as shown in Figure-3, and the yield was found to be 8.32%.

Refractive Index of star anise essential oil.

The refractive index of star anise essential oil was found to be 1.5037.

Density.

The density of the star anise oil was recorded to be 0.98 g/cm3 at 24.2°C.

Fourier-transform infrared spectroscopy (FTIR) of Anise oil essential oil.

Star anise EO showed the CH2 peak at 723 cm-1, C=C at 1641 cm-1, C-O at 1247 cm-1, C-C at cm-1, C=O at 1737 cm-1, C-H st at 2845 cm-1, C-H st at 2830 cm-1, 2925 cm-1, and 2926 cm-1. O-H st at 3125 cm-1, alcoholic OH at 3400-3700 cm-1, OH bend at 947 cm-1, OH bend at 1418 cm-1, C-O at 1244 cm-1, Ar- C-H def at 1127 cm-1, as shown in Figure-4.

Calibration curve by UV-visible spectroscopy.

The line equation was found to be $y = 0.6982x + 0.0472$, and R^2 value was 0.9998, as shown in Table-2 and Figure-5.

Drug excipient interaction.

A study of star anise volatile oil-based nano-emulsion showed no drug excipient interaction (Hadel A. Abo El-Enin et.al., 2022). The FTIR of Tween-80 showed C-H stretching 2929 cm-1, 1731 cm-1 strong C=O stretching, C=C at 1640 cm-1, C-O st at 1107 cm-1, C-O st at 1097 cm-1, C=C bending at 794 cm-1, as shown in Figure-6. The FTIR of PEG-200 and PEG-300 showed C-H peak at 2931 cm-1, C=O st at 1770 cm-1, C-O st at 1142 cm-1 and 1077 cm-1, and C-H bend at 880 cm-1, as shown in Figure-6. FTIR spectrum of star anise oil-based nano-emulsion showed the presence of Ar- C-H def at 1127 cm-1, C=C at 1640 cm-1, C=C bending at 794 cm-1, C=O at 1737 cm-1, C-H bend at 880 cm-1, C-H peak at 2931 cm-1, C-H st at 2845 cm-1, C-H stretching 2929 cm-1, CH2 peak at 723 cm-1, C-O at 1244 cm-1, C-O at 1247 cm-1, C-O st at 1097 cm-1, C-O st at 1107 cm-1, C-O st at 1142 cm-1 and 1077 cm-1, OH alcoholic at 3400-3700 cm-1, OH bend at 1418 cm-1, OH bend at 947 cm-1, O-H st at 3125 cm-1, as shown in Figure-7.

Preparation of nano-emulsion from star anise oil.

All sixteen batches of nano emulsions (homogenization and ultrasonication method) were prepared, as shown in Figure 8.

Evaluation of nano-emulsion.

Various parameters like yield, refractive index, FTIR, drug content, drug release studies, drug release kinetics, and stability studies were conducted.

Yield.

The yield varied from 99.94-99.99 %, as shown in Table-3.

Refractive Index.

The refractive index of the nano-emulsions prepared by the homogenization method varied from 1.4792-1.4874, while nano-emulsions prepared by the ultrasonication method ranged from 1.4814-1.4867 for nano-emulsion batch NE-CH, NE-GH, NE-ES, and NE-BS, respectively, at 23.8°C, as shown in Figure-9. The nano-emulsions prepared by the homogenization method showed a higher refractive index than nano-emulsions prepared by the ultrasonication method, as shown in Table-3. A nano emulsion-based study (Dasgupta et al, 2014) also showed no significant effect on the refractive index.

pH analysis.

pH test was carried out in triplicate at 25°C, and as shown in the table, the pH range is indicated between 6.8-7.2, NEBH, and NEFH, as shown in Table-3, which is normal and can be applied to the skin (Ghareeb, 2020).

Particle size analysis.

The particle of all 16 batches were measured that showed the least particle size 646.1±71.54 nm (NE-HH batch) 2851±408.4 nm (NE-DH batch) by the homogenization method, 694±195.48 nm (NE-HS batch) to 2646±1036.2 nm (NE-FS batch) by the sonication method (Rashid et al., 2023), as shown in Figure-10, Figure-11, Figure-12. Particle size has been assessed using a particle size analyzer (PAAR Anton Litesizer) which analyzed fluctuations due to Brownian motion. Among batches NE-AH, NE-BH, NE-AS, NE-BS, the NE-BH and NE-BS showed an increase in particle size due to the use of PEG-300 rather than the use of PEG-200. The batch NE-EH, NE-FH, and NE-ES, NE-FS, the NE-EH and NH-FS showed an increase in particle size NE-EH due to PEG-200 increase in NH-FS due to PEG-300. The batch NE-GH, NE-HH, and NE-GS, NE-HS showed an increase in particle size in NE-GS due to the use of PEG-200 in the case of

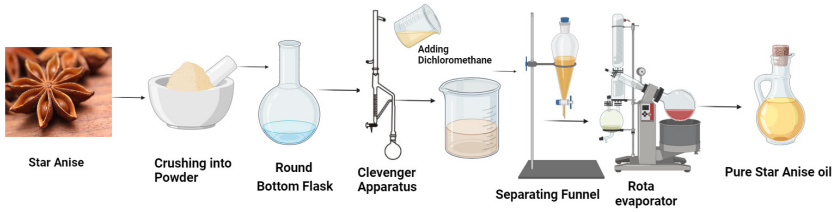

Figure 1. Extraction and purification of essential oil from star anise fruit

Table 1. Composition of nano-emulsion

Ingredients	NE-A H/S	NE-B H/S	NE-C H/S	NE-D H/S	NE-E H/S	NE-F H/S	NE-G H/S	NE-H H/S
Oil (anise oil, mL)	2	2	2	2	2	2	2	2
Surfactant (Tween-80, mL)	1.5	1.5	1	1	1	1	2	2
Co-surfactant-1 (PEG-200, mL)	1.5	0	1.5	0.5	2	0	1	0
Co-surfactant-2 PEG-300, mL)	0	1.5	0.5	1.5	0	2	0	1
Total (mL)	5	5	5	5	5	5	5	5

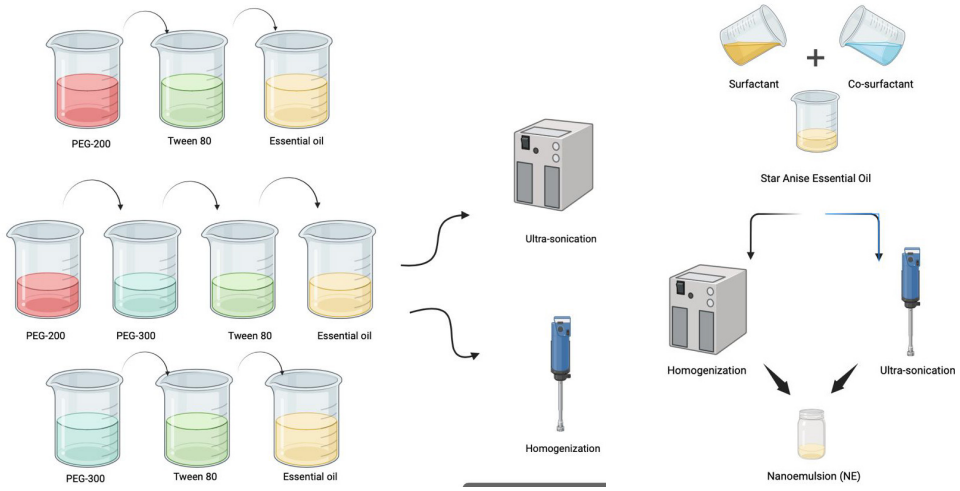

Figure 2. Formulation of nano-emulsion

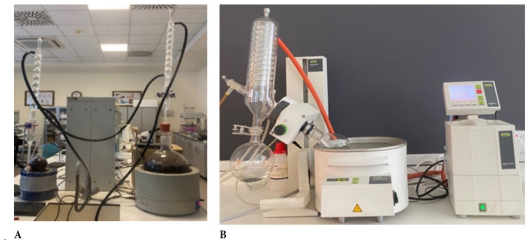

Figure 3. Star Anise oil essential oil (A) Extraction, (B) Purification

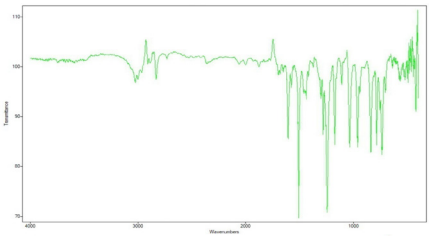

Figure 4. FTIR of Star anise essential oil

Table 2. UV-visible spectroscopy data of star anise essential oil

Concentration (µg/mL)	**Absorbance**
X	**Y**
20	0.757
40	1.423
60	2.163
80	2.823
100	3.534
120	4.246

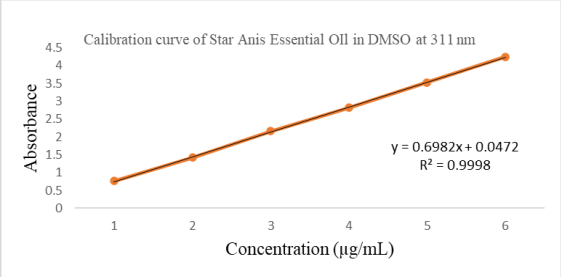

Figure 5. UV-visible spectroscopy curve of star anise essential oil

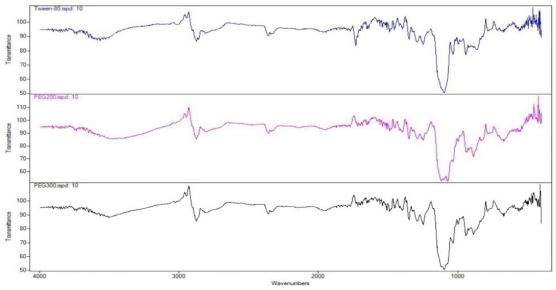

Figure 6. FTIR of (A) Tween-80, (B) PEG-200, (C) PEG-300

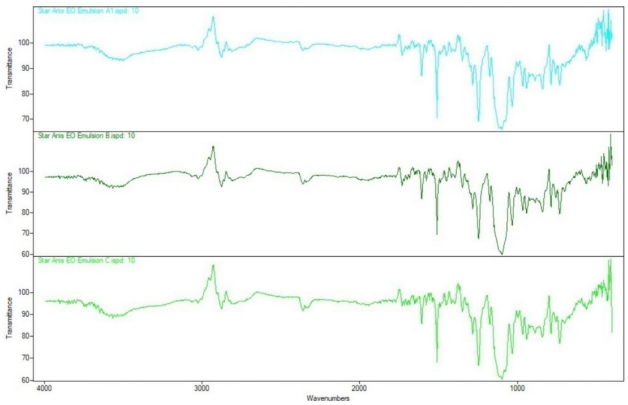

Figure 7. FTIR of nano-emulsion

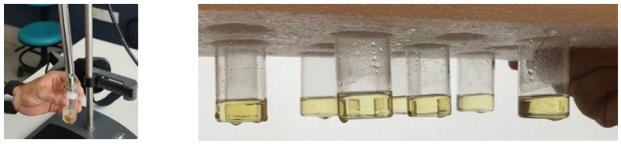

Figure 8. Nano-emulsion from Star Anise Oil (A) Homogenization, (B) Ultrasonication

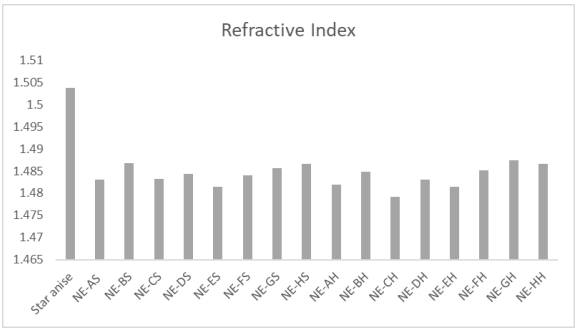

Figure 9. Refractive index of the samples

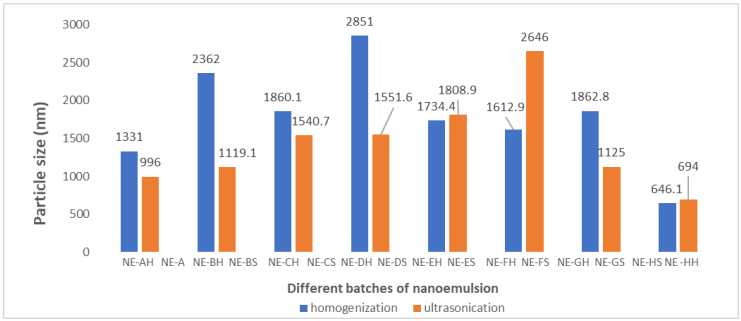

Figure 10. Droplet size of nano-emulsion batches

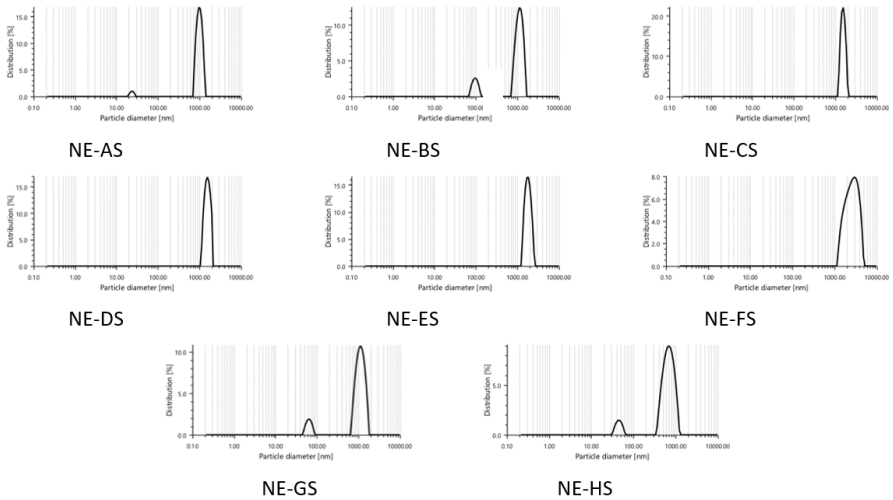

Figure 12. Droplet size of nano-emulsion by ultrasonication

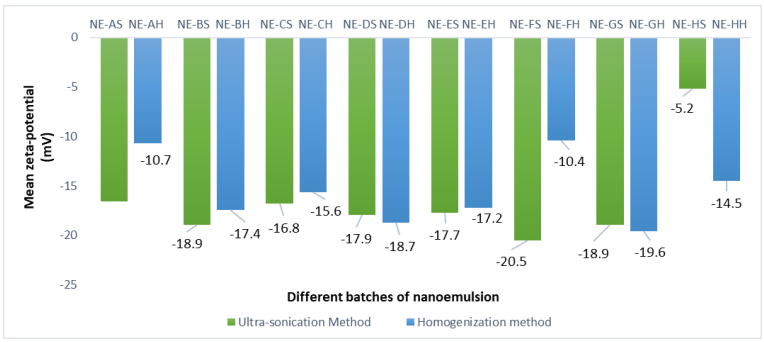

Figure 13. Zeta potential of nano-emulsion batches.

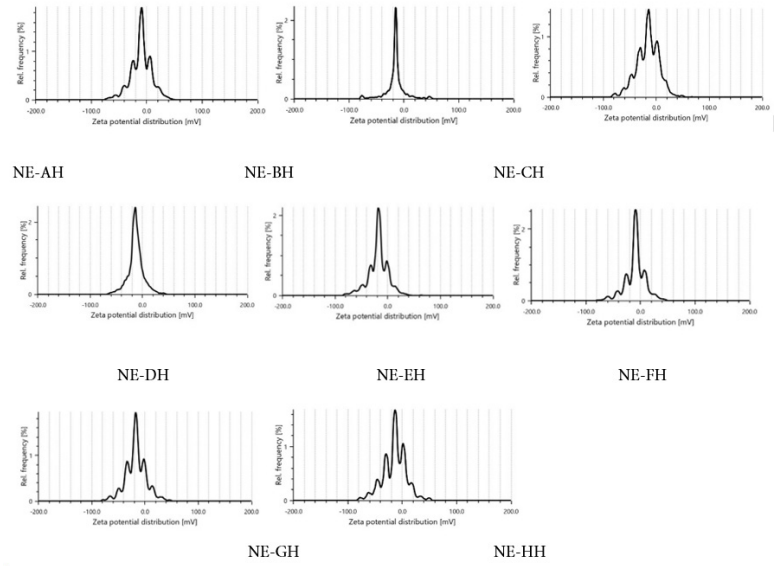

Figure-14. Zeta potential by Homogenization method

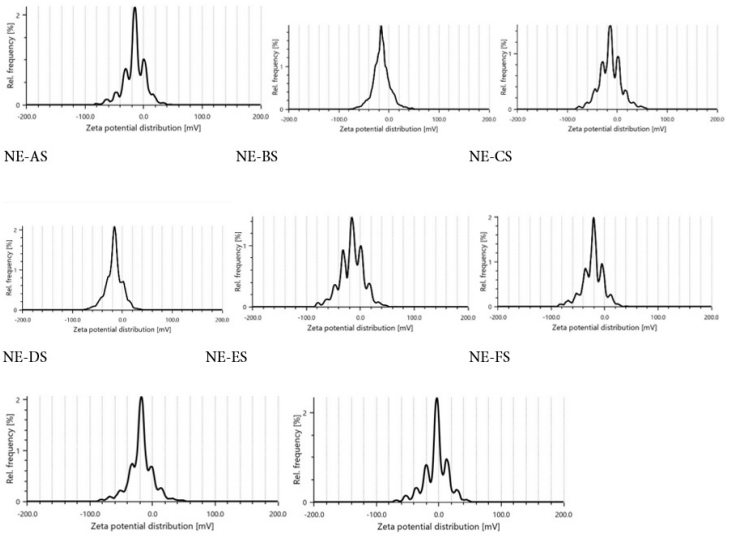

Figure-15. Zeta potential by Ultrasonication method

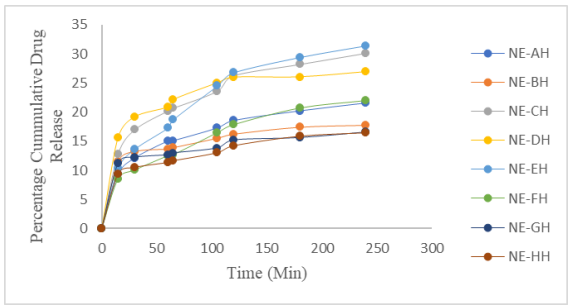

Figure 16. Drug release of nano-emulsion batches by homogenization

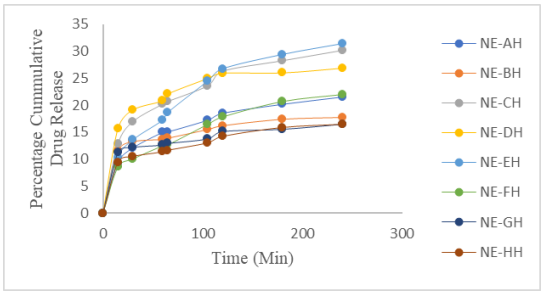

Figure 17. Drug release of nano-emulsion batches by ultrasonication

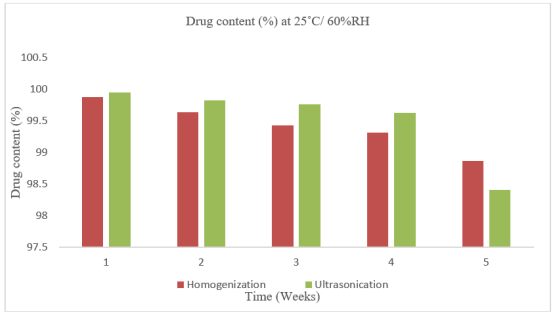

Figure 18. Drug content of nano-emulsion in stability studies

Table 3. Yield, refractive Index, pH, particle size, zeta potential, drug content of nano-emulsion batches

Method of preparation	NE Batches	Yield	Refractive Index	pH	Particle Size (nm)	Zeta potential(mV)	Drug content (%)
Homogenization	1. NE-AH	99.98	1.4819	6.9	1331±256.8	-10.7	98.64±0.34
	2. NE-BH	99.95	1.4848	6.8	2362±482.4	-17.4	98.65±0.45
	3. NE-CH	99.96	1.4792	7	1860.1±444.7	-15.6	97.56±0.34
	4. NE-DH	99.98	1.483	6.8	2851±408.4	-18.7	98.45±0.35
	5. NE-EH	99.94	1.4814	7.1	1734.4±237	-17.2	98.67±0.75
	6. NE-FH	99.98	1.4851	7.2	1612.9±206.2	-10.4	99.23±0.21
	7. NE-GH	99.97	1.4874	7	1862.8±412	-19.6	98.67±0.54
	8. NE-HH	99.99	1.4866	7.1	646.1±71.54	-14.5	99.34±0.42
Ultrasonication	9. NE-AS	99.98	1.483	7.2	996±147.57	-16.6	99.56±0.25
	10. NE-BS	99.95	1.4867	6.9	1119.1±213	-18.9	98.56±0.75
	11. NE-CS	99.97	1.4832	7	1540.7±244.4	-16.8	99.44±0.14
	12. NE-DS	99.96	1.4843	7.2	1551.6±244.4	-17.9	98.78±0.56
	13. NE-ES	99.95	1.4814	6.8	1808.9±301	-17.7	99.67±0.34
	14. NE-FS	99.99	1.484	7	2646±1036.2	-20.5	99.12±0.56
	15. NE-GS	99.97	1.4856	7.1	1125±257.5	-18.9	98.56±0.33
	16. NE-HS	99.98	1.4866	6.9	694±195.48	-5.2	98.23±0.45

Table 4. Drug release of nano-emulsion batches by homogenization

Min	NE-A-H	NE-B-H	NE-C-H	NE-D-H	NE-E-H	NE-F-H	NE-G-H	NE-H-H
0	0	0	0	0	0	0	0	0
15	9.298±1.23	11.526±0.54	12.815±0.54	15.673±0.65	10.308±1.34	8.582±1.45	11.246±1.54	9.434±1.42
30	12.113±1.63	13.259±1.23	16.97±1.86	19.169±1.23	13.61±1.45	10.093±1.13	12.235±0.65	10.523±1.43
60	15.014±1.15	13.682±1.75	20.201±0.36	20.845±1.45	17.256±0.35	12.529±1.24	12.658±1.43	11.368±0.25
65	15.086±0.43	13.904±1.37	20.681±1.47	22.113±0.26	18.689±1.14	12.701±0.35	12.966±1.35	11.662±1.33
105	17.256±1.17	15.523±1.65	23.596±1.15	24.986±1.37	24.484±1.35	16.519±0.25	13.818±0.25	13.037±0.63
120	18.539±1.37	16.218±0.87	26.275±1.33	25.967±1.34	26.777±1.43	17.894±1.75	15.186±1.24	14.234±1.34
180	20.201±0.28	17.414±1.25	28.223±0.65	26.024±1.65	29.413±0.53	20.752±1.36	15.595±0.65	15.867±1.62
240	21.54±1.11	17.751±0.97	30.129±1.21	26.898±0.33	31.411±1.26	22.042±1.64	16.54±1.36	16.461±1.23

Table 5. Drug release of nano-emulsion batches by ultrasonication

Min	NE-A-S	NE-B-S	NE-C-S	NE-D-S	NE-E-S	NE-F-S	NE-G-S	NE-H-S
0	0	0	0	0	0	0	0	0
15	11.082±1.34	11.748±1.12	5.924±1.23	9.943±1.43	9.284±0.23	8.438±1.43	8.854±0.43	8.66±0.75
30	14.864±0.54	13.195±0.34	9.613±1.11	12.228±0.74	12.45±0.64	13.095±0.23	11.511±1.24	10.1±0.35
60	16.597±1.64	13.897±1.56	13.181±0.43	15.731±0.76	17.185±1.34	19.248±0.35	12.256±0.52	12.163±1.23
65	16.841±0.26	14.549±1.74	13.811±0.32	16.239±1.45	20.043±1.65	19.713±0.26	12.428±1.14	12.543±0.43
105	17.815±1.43	16.519±0.24	18.703±1.47	19.241±1.24	25.852±0.27	21.361±1.16	14.235±0.44	14.319±0.56
120	18.596±1.53	17.6±1.75	21.49±1.75	20.688±0.11	27.572±0.58	22.113±1.45	15.017±0.45	15.029±1.34
180	19.706±1.32	19.334±0.35	24.477±0.34	23.123±1.34	30.795±1.16	24.004±0.36	16.64±1.26	15.824±0.54
240	20.043±0.21	19.807±1.23	25.351±1.57	24.191±0.45	34.004±1.74	24.026±0.64	17.328±0.42	16.619±1.26

Table 6. Drug release kinetics of best nano-emulsion batches prepared by homogenization and sonication method.

	NE-EH		NE-ES	
Model Fitting	**R^2**	**K**	**R^2**	**k**
Zero order	0.8262	0.1159	0.8573	0.1291
First order	0.8643	-0.0014	0.8947	-0.0016
Higuchi Matrix	0.9110	5.6204	0.9099	5.8902
Peppas	0.9850	1.6633	0.9847	1.4704
Hix.Crow.	0.8521	0.0004	0.8828	0.0005
Parameters for Korsmeyer-Peppas Equation				
N	0.4250		0.4932	
K	1.6633		1.4704	
Best fit model	Peppas Korsmeyer		Peppas Korsmeyer	
Mechanism of release	Fickian Diffusion (Higuchi Matrix)		Fickian Diffusion (Higuchi Matrix)	

Table 7. Drug content of nano-emulsion in stability studies

Time (Weeks)	Drug content (%) at 25°C/ 60%RH	
	NEEH	NEES
1	99.87±0.12	99.95±0.34
2	99.63±0.25	99.82±0.13
3	99.42±0.32	99.76±0.21
4	99.31±0.39	99.62±0.32
5	98.86±0.25	98.41±0.23

NH-HS due to the use of PEG-300. The batch NE-EH, NE-GH, and NE-ES, NE-GS showed an increase in particle size NE-EH use more amounts of PEG-200, but NE-GS use fewer amounts of PEG-200. The batch NE-AH, NE-GH, and NE-AS, NE-GS showed an increase in particle size NE-GH and NE-GS due to more amounts of Tween-80. The batch NE-AH, NE-AH, and NE-BS, NE-BS, the particle size increased in both NE-BH, NE-BS more amount of PEG-300 than PEG-200, as shown in Table-3. A study showed an increase in the size of the nanoemulsion on increasing the amount of Tween 80 (Hanafi and Amani, 2021).

Zeta potential.

The zeta potential of all 16 batches was measured that showed the least zeta potential value -10.4 (NE-FH batch) to -19.6 (NE-GH batch) by the homogenization method, -5.2 (NE-HS batches) to -20.5 (NE-FS batch) by the sonication method, as shown in Table-3 and Figure-13, Figure-14, Figure-15. Among batch NE-AH, NE-BH, NE-AS, NE-BS, the NE-BH and NE-BS showed an increase in particle size due to the use of PEG-300 rather than the use of PEG-200. The batch NE-EH, NE-FH, and NE-ES, NE-FS, the NE-EH and NH-FS showed an increase in zeta potential NE-EH due to the use of PEG-200 in the case of NH-FS due to the use of PEG-300. The batch NE-GH, NE-HH, and NE-GS, NE-HS showed an increase in zeta potential in NE-GS due to the use of PEG-200 in the case of NH-HS due to the use of PEG-300. The batch NE-EH, NE-GH, and NE-ES, NE-GS showed an increase zeta potential NE-EH use more amount of PEG-200, but NE-ES use fewer amounts of PEG-200. The batch NE-AH, NE-GH, and NE-AS, NE-GS showed an increase in zeta potential NE-GH and NE-GS due to more amounts of Tween-80. The batch NE-AH, NE-AH, and NE-BS, NE-BS, the zeta potential in both NE-BH, NE-BS more amount of PEG-300 than PEG-200. A study showed the change in zeta potential on the use of surfactants in different ratios (Maharini et.al., 2018).

Homogenization.

After finding the Zeta potential of the nano-emulsions prepared by the homogenization method, which coded as NE-AH, NE-BH, NE-CH, NE-DH, NE-EH, NE-FH, NE-GH, and NE-HH. It showed that the mean zeta potential of the batches prepared by the homogenization method was -15.0 mV. The range of zeta-potential values for these batches was -10.7 mV to -19.6 mV. Among these batches, batch NE-GH showed the highest zeta potential of -19.6 mV, while batch NE-FH had the lowest zeta potential of -10.4 mV, as shown in Table-3.

Ultrasonication.

On the other hand, for the batches prepared using the ultrasonication method coded as NE-AS, NE-BS, NE-CS, NE-DS, NE-ES, NE-FS, NE-GS, and NE-HS, the mean zeta potential was -16.5625 mV, with a range of -5.2 mV to -20.5 mV. Among these batches, batch NE-FS displayed the highest zeta potential of -20.5 mV, while batch NE-HS had the lowest zeta potential of -5.2 mV, as shown in Table-3.

Drug content.

The drug content of all 16 batches measured that showed the least value 97.56±0.34% (NE-CH batch) to 99.34±0.42% (NE-HH batch) by the homogenization method, 98.23±0.45% (NE-HS batch) to 99.67±0.34% (NE-ES batch) by the sonication method, as shown in Table-3.

Drug release.

Among the drug release of all 16 batches, the batch NE-HH prepared by homogenization method showed the least drug release NEHH 16.461±1.23% due to 2 mL Tween-80 with 1 mL PEG-300, while the maximum amount of drug release was NEEH 31.411±1.26% showed by NE-EH due to 1 mL Tween-80 with 2 mL PEG-200, as shown in Table 4 and Figure-16. The batch NE-HS prepared by ultrasonication method showed the least drug release NEHS 16.619±1.26% due to 2 mL Tween-80 with 1 mL PEG-300, while the maximum amount of drug release was NEES 34.004±1.74% showed by NE-ES due to 1 mL Tween-80 with 2 mL PEG-200, as shown in Table 5 and Figure-17.

Drug release kinetics.

The nano-emulsion batch NE-EH and NE-ES showed Peppas Korsmeyer as the best fit model and Fickian Diffusion (Higuchi Matrix) was mechanism of release as showed in **Table-6**.

Stability.

The drug content of best selected nano-emulsion batches prepared by homogenization method and ultrasonication method found to be 98.86±0.25% and 98.41±0.23% up to 5 weeks at 25˚C/ 60%RH in stability studies as showed in **Table-7 and Figure-18**.

Discussion

The exploration of the medicinal properties of plants is an age-old practice deeply rooted in human history. In the current context of escalating health concerns, it shows the potential health benefits of star anise, specifically its volatile oil, which is reputed for its efficacy against various health issues such as bronchitis, colds, flu, indigestion, facial paralysis, and intestinal cramps.

Star anise (*Illicium verum*) is recognized for its medicinal properties, particularly the efficacy of its volatile oil against various health issues such as bronchitis, colds, flu, indigestion, facial paralysis, and intestinal cramps. This properties are essential to formulate and assess the nano-emulsion of the oil to harness and enhance the therapeutic potential of star anise volatile oil. Nano-emulsions are colloidal dispersions with droplet sizes in the nanometer range, which can offer improved stability and prolonged drug release compared to conventional emulsions.

Our result revealed that the smallest droplet sizes were observed in specific batches prepared by homogenization (NE-HH) and

ultrasonication (NE-HS). Both batches also exhibited the least zeta potential values, indicating good stability. The highest drug release percentages were recorded in certain batches, with NE-EH and NE-ES showing the best performance. Both of these batches followed the Peppas Korsmeyer model, and the release mechanism was identified as Fickian Diffusion (Higuchi Matrix). Our result successfully demonstrated the formulation of star anise volatile oil nano-emulsions using homogenization and ultrasonication methods. The characterized nano-emulsions displayed good stability, prolonged drug release, and promising drug release kinetics. The essential oil extracted from star anise is further used to formulate nano-emulsions. The formulations involve various components such as Tween-80, PEG-200, and PEG-300. Two methods, homogenization and ultrasonication, were employed to prepare the nano-emulsions. The resulting formulations were then subjected to a comprehensive characterization and evaluation process, including refractive index, pH determination, FTIR, particle size analysis, zeta potential measurement, drug content determination, drug release studies, drug release kinetics, and stability studies. The results indicated the successful extraction and purification of star anise oil, yielding 8.32%. The characterization of the extracted oil revealed specific values for refractive index, density, and FTIR spectrum, which confirms the presence of various functional groups. The UV-visible spectroscopy established a calibration curve for drug concentration and absorbance.

The preparation of nano-emulsions involved careful consideration of the composition and method used. We evaluated various parameters for the nano-emulsions, including refractive index, pH, particle size, zeta potential, drug content, drug release, drug release kinetics, and stability. Notably, the choice of surfactants and co-surfactants, as well as their ratios, influenced the particle size and zeta potential of the nano-emulsions.

The method of preparation and the composition of the formulations significantly changed the particle size of star anise nano-emulsions. Ultrasonication consistently produced smaller particle sizes due to the intense energy input, while each ingredient, especially co-surfactants, played a nuanced role in determining particle size. The interaction between co-surfactants, their concentrations, and their synergistic effects further influenced particle size. Meanwhile, the homogenization method involved mechanical agitation and high shear forces, which might have influenced the surface charge distribution of the droplets in the nano-emulsion.

Furthermore, the zeta potential values showed considerable variability within each method. For instance, the homogenization method showed a zeta potential range from -10.4 mV to -19.6 mV, while the ultrasonication method showed a range from -5.2 mV to -20.5 mV. This broad distribution of zeta potential values might be attributed to variations in formulation compositions and particle size distributions, or inherent fluctuations in the processing conditions, which could have influenced the surface charge and interactions between droplets.

The result demonstrated that the ultrasonication method consistently produces smaller particle sizes, while the homogenization method showed a broader distribution of zeta potential values. The stability studies conducted over five weeks at 25°C/60% RH indicated the robustness of the selected nano-emulsion batches.

Conclsuion

In conclsuion, our study provided valuable insights into star anise oil-based nano-emulsions' extraction, purification, and formulation processes. The comprehensive characterization and evaluation shed light on the impact of formulation components and methods on nano-emulsions' properties. The findings contribute to understanding the complex interplay between ingredients and processing conditions, which is crucial for optimizing the formulation of nano-emulsions for various applications.

Author contribution

S.V. prepared study design, S.S.S., B.A.I., D.I.I., S.F..A., O.P. conceptualized, perfomed experimental and data analsyis

Acknowledgment

The authors thank the management of TIU to provide every facility for the conduct of this research.

Competing financial interests

The authors have no conflict of interest.

References

Alaayedi, M. H., & Maraie, N. K. (2023). Lomustine's nanoemulsion as nose-to-brain drug delivery system for CNS tumor treatment. Saudi Pharmaceutical Journal . SPJ . the official publication of the Saudi Pharmaceutical Society, 31(8), 101692. https.//doi.org/10.1016/j.jsps.2023.06.025

AlBalawi, A. N., Elmetwalli, A., Baraka, D. M., Alnagar, H. A., Alamri, E. S., & Hassan, M. G. (2023). Chemical Constituents, Antioxidant Potential, and Antimicrobial Efficacy of Pimpinella anisum Extracts against Multidrug-Resistant Bacteria. Microorganisms, 11(4),1024. https.//doi.org/10.3390/microorganisms11041024

Alhamdany, A.T., Saeed, A. M. H., & Alaayedi, M. (2021). Nanoemulsion and Solid Nanoemulsion for Improving Oral Delivery of a Breast Cancer Drug. Formulation, Evaluation, and a Comparison Study. Saudi pharmaceutical journal. SPJ . the official publication of the Saudi Pharmaceutical Society, 29(11), 1278–1288.

Barbouchi, M., & Benzidia, B. (2021). Chemical variability in essential oils isolated from roots, stems, leaves and flowers of three Ruta species growing in Morocco. Journal of King Saud University-Science, 33(8), 101634.

Bayan, M. F., Jaradat, A., Alyami, M. H., Naser, A. Y. (2023). Smart Pellets for Controlled Delivery of 5-Fluorouracil.Molecules. 28(1). 306.doi. 10.3390/molecules28010306.

Brahmi, F., Mokhtari, O., Legssyer, B., Hamdani, I., Asehraou, A., Hasnaoui, I., ... & Tahani, A. (2021). Chemical and biological characterization of essential oils extracted from citrus fruits peels. Materials Today. Proceedings, 45, 7794-7799.

Chopra, H., Bibi, S., Goyal, R., Gautam, R. K., Trivedi, R., Upadhyay, T. K., ... & Kim, B. (2022). Chemopreventive potential of dietary nanonutraceuticals for prostate cancer. an extensive review. Frontiers in Oncology, 2941.

Dasgupta, S., Ghosh, S. K., Ray, S., Kaurav, S. S., Mazumder, B. (2014). In vitro & in vivo Studies on Lornoxicam Loaded Nanoemulsion Gels for Topical Application. Current Drug Delivery, 11, 132-138

Dinache, A., Tozar, T., Smarandache, A., Andrei, I. R., Nistorescu, S., Nastasa, V., & Romanitan, M. O. (2020). Spectroscopic characterization of emulsions generated with a new laser-assisted device. Molecules, 25(7), 1729.

Elkordy, A. A., Haj-Ahmad, R. R., Awaad, A. S., & Zaki, R. M. (2021). An overview on natural product drug formulations from conventional medicines to nanomedicines. Past, present and future. Journal of Drug Delivery Science and Technology, 63, 102459.

Getahun, T., Sharma, V., & Gupta, N. (2020). Chemical composition, antibacterial and antioxidant activities of oils obtained by different extraction methods from Lepidium sativum L. seeds. Industrial Crops and Products, 156, 112876.

Ghareeb, M. M. (2020). Formulation and characterization of isradipine as oral nanoemulsion. Iraqi Journal of Pharmaceutical Sciences (P-ISSN 1683-3597 E-ISSN 2521-3512), 29(1), 143-153.

Habeeb, H., & Thoppil, J. E. (2022). Medicinal herbs as a panacea for biogenic silver nanoparticles. Bulletin of the National Research Centre, 46(1), 9.

Hanafi A., Amani A., (2021). Effect of Processing/Formulation Parameters on Particle Size of Nanoemulsions Containing Ibuprofen - An Artificial Neural Networks Study, Pharmaceutical Sciences, 27(2), 230-237 doi.10.34172/PS.2020.74

Kolani, L., Nadio, N. A., Bokobana, E. M., Koba, K., Raynaud, C., & Sanda, K. (2022). Physico-Chemical Attributes of Essential Oil from Zingiber officinale Roscoe and Zingiber zerumbet (L.) Smith Cultivars Grown in Togo. American Journal of Plant Sciences, 13(11), 1360-1372..

Liang, D., Wang, C., Luo, X., Wang, Z., Kong, F., & Bi, Y. (2023). Preparation, characterization and properties of cinnamon essential oil nano-emulsion formed by different emulsifiers. Journal of Drug Delivery Science and Technology, 104638.

Liao, Z., Huang, Q., Cheng, Q., Khan, S., Yu, X. (2021). Seasonal Variation in Chemical Compositions of Essential Oils Extracted from Lavandin Flowers in the Yun-Gui Plateau of China. Molecules. 17;26(18).5639. doi. 10.3390/molecules26185639.

Maharini, I., Utami, D. T. and Fitrianingsih. (2018). The Influence of Tween 80 in The Formulation of Nano emulsion Virgin Coconut Oil. International Conference on Pharmaceutical Research and Practice ISBN. 978-979-98417-5-9 | Universitas Islam Indonesia.

Mahmod, M. R., Junayed, A., Bhowmick, C., Sompa, S., Sultana, T., Akter, T., & Sikder, M. A. (2021). Antibacterial activity of silver nanoparticles synthesized from leaf and flower extracts of Galinsoga formosa. J. Adv. Biotechnol. Exp. Ther, 4(2), 178-186.

Majali, I. S. (2022). Antioxidant and Anti-Inflammatory Activity of Star Anise (Illicium Verum) in Murine Model. Biomedical and Pharmacology Journal, 15(2), 1097-1108.

Manzoor, M., Sharma, P., Murtaza, M., Jaiswal, A. K., & Jaglan, S. (2023). Fabrication, characterization, and interventions of protein, polysaccharide and lipid-based nanoemulsions in food and nutraceutical delivery applications. A review. International Journal of Biological Macromolecules, 124485..

Miljanović, A. Dent, M., Grbin, D., Pedisić, S., Zorić, Z., Marijanović, Z., Jerković, I., Bielen, A. (2023). Sage, Rosemary, and Bay Laurel Hydrodistillation By-Products as a Source of Bioactive Compounds. Plants. 12(13), 2394; https.//doi.org/10.3390/plants12132394.

Miranda, F. A. S., Iftitah, E. D., Warsito, W., Berliana, A. N. I., & Seta, F. A. (2022). Continuous Essential Oil and Oleoresin Extraction from Star Anise (Illicium verum) by Hydrodistillation and Solvent Extraction. The Indonesian Green Technology Journal, 11(2).

Patil, A. S., Li, X., & Xu, Y. (2023). Simultaneous determination of three curative flavonoids and neurotoxic anisatin in star anise fruits by ultra-high performance liquid chromatography-tandem mass spectrometry. Food chemistry, 429, 136769. https.//doi.org/10.1016/j.foodchem.2023.136769

Pires, P. C., Fernandes, M., Nina, F., Gama, F., Gomes, M. F., Rodrigues, L. E., & Santos, A. O. (2023). Innovative Aqueous Nanoemulsion Prepared by Phase Inversion Emulsification with Exceptional Homogeneity. Pharmaceutics, 15(7), 1878.

Pratap-Singh, A., Guo, Y., Lara Ochoa, S., Fathordoobady, F., & Singh, A. (2021). Optimal ultrasonication process time remains constant for a specific nanoemulsion size reduction system. Scientific reports, 11(1), 9241. https.//doi.org/10.1038/s41598-021-87642-9.

Rani V, Rajan KR., Bhupathyraaj S., Priya M, Halligudi R.K.N., Al-Ghazali, M. A., & Pol, P. D. (2022). The effect of polymers on drug release kinetics in nanoemulsion in situ gel formulation. Polymers, 14(3), 427.

Rashid, A., Qayum, A., Liang, Q., Kang, L., Raza, H., Chi, Z., & Ma, H. (2023). Preparation and characterization of ultrasound-assisted essential oil-loaded nanoemulsions stimulated pullulan-based bioactive film for strawberry fruit preservation. Food Chemistry, 422, 136254.

Roberts, J., Power, A., Chapman, J., Chandra, S., & Cozzolino, D. (2018). The use of UV-Vis spectroscopy in bioprocess and fermentation monitoring. Fermentation, 4(1), 18.

Salem, M. A., El-Shiekh, R. A., Hashem, R. A., & Hassan, M. (2021). In vivo antibacterial activity of star anise (Illicium verum Hook.) Extract Using Murine MRSA skin infection model in relation to its metabolite profile. Infection and Drug Resistance, 33-48.

Salem, M.A., El-Shiekh, R. A., Hashem, R. A., Hassan, M. (2021). In vivo Antibacterial Activity of Star Anise (Illicium verum Hook.) Extract Using Murine MRSA

Skin Infection Model in Relation to Its Metabolite Profile. Infect Drug Resist. 6.14.33-48. doi. 10.2147/IDR.S285940. eCollection 2021.

Sharafan, M., Jafernik, K., Ekiert, H., Kubica, P., Kocjan, R., Blicharska, E., Szopa, A. (2022). Illicium verum (Star Anise) and Trans-Anethole as Valuable Raw Materials for Medicinal and Cosmetic Applications, Molecules. 27(3), 650; https.//doi.org/10.3390/molecules27030650.

Srivastava, S., He, F., Huang, Y., Niu, M., Adholeya, A., & Peng, W. K. (2023). A Brief Review on Medicinal Plants-At-Arms against COVID-19. Interdisciplinary Perspectives on Infectious Diseases, 2023.

Sukasri, A., Utomo, W. B., Sjafruddin, R., Nursam, M. (2023). The Use of Soxhlet Techniques in the Essential Oil Extraction from Anise Seeds (Pimpinella anisum). Equilibrium Journal of Chemical Engineering. 7(1).59. DOI. 10.20961/equilibrium.v7i1.73410.

Vilanculos, J. R. Z., de Farias, B. S., Engelmann, J. I., Ribeiro, E. S., de Oliveira, P. D., Cadaval Jr, T. R. S. A., & de Almeida Pinto, L. A. (2023). Physicochemical evaluation of chitosan–xanthan gum nanoemulsions as polyunsaturated enriched lipid–carrier. Journal of Molecular Liquids, 386, 122533.

Visht, S., & Kulkarni, G.T. (2016). Glycyrrhetinic Acid Ammonium Loaded Microspheres Using Colocasia esculenta and Bombax ceiba mucilages. In Vitro and In Vivo Characterization. Current Drug Therapy, 11(2), 101-114.

Visht, S., & Sirwan Salih, S. (2023). Effect of Cholesterol and Different Solvents on Particle Size, Zeta Potential and Drug Release of Eucalyptus Oil Phytosome. Pharmacognosy Research, 15(3).

Zerkani, H., Amalich, S., Tagnaout, I., Bouharroud, R., & Zair, T. (2022). Chemical composition, pharmaceutical potential and toxicity of the essential oils extracted from the leaves, fruits and barks of Pistacia atlantica. Biocatalysis and Agricultural Biotechnology, 43, 102431.

Zhang, Q., Zhang, C., Luo, X., Wang, Z., Guo, J., & Bi, Y. (2022). Protein stabilized seabuckthorn fruit oil Nanoemulsion. Preparation, characterization and performance research. Food Bioscience, 46, 101597.

Zhang, R., Luo, L., Yang, Z., Ashokkumar, M., & Hemar, Y. (2021). Formation by high power ultrasound of aggregated emulsions stabilised with milk protein concentrate (MPC70). Ultrasonics Sonochemistry, 81, 105852.

Zou, Q., Huang, Y., Zhang, W., Lu, C., & Yuan, J. (2023). A Comprehensive Review of the Pharmacology, Chemistry, Traditional Uses and Quality Control of Star Anise (Illicium verum Hook. F.). An Aromatic Medicinal Plant. Molecules, 28(21), 7378.